CCFE-PR(16)12

M. Fitzgerald, S.E. Sharapov, P. Rodrigues, D. Borba

Predictive Nonlinear Studies of TAE-Induced Alpha-Particle Transport in the Q=10 ITER Baseline Scenario

Predictive Nonlinear Studies of TAE-Induced Alpha-Particle Transport in the Q=10 ITER Baseline Scenario

M. Fitzgerald[1], S.E. Sharapov[1], P. Rodrigues[2], D. Borba[2]

[1]Culham Centre for Fusion Energy, Culham Science Centre, Abingdon OX14 3DB, UK
[2]Instituto de Plasmas e Fus~ao Nuclear, Instituto Superior Tecnico, Universidade de Lisboa, 1049-001 Lisboa, Portugal

Predictive nonlinear studies of TAE-induced alpha-particle transport in the Q=10 ITER baseline scenario

Abstract. We use the HAGIS code to compute the nonlinear stability of the Q=10 ITER baseline scenario to toroidal Alfvéneigenmodes (TAE) and the subsequent effects of these modes on fusion alpha-particle redistribution. Our calculations build upon an earlier linear stability survey [Rodrigues, P. et al. (2015). Nuclear Fusion, 55(8), 083003] which provides accurate values of bulk ion, impurity ion and electron thermal Landau damping for our HAGIS calculations. Nonlinear calculations of up to 129 coupled TAEs with toroidal mode numbers in the range n=1-35 have been performed. The effects of frequency sweeping were also included to examine possible phase space hole and clump convective transport. We find that even parity core localised modes are dominant (expected from linear theory), and that linearly stable global modes are destabilised nonlinearly. Landau damping is found to be important in reducing saturation amplitudes of coupled modes to below $\delta B_r/B_0 \sim 3 \times 10^{-4}$. For these amplitudes, stochastic transport of alpha-particles occurs in a narrow region where predominantly core localised modes are found, implying the formation of a transport barrier at $r/a \approx 0.5$, beyond which, the weakly driven global modes are found. We find that for flat q profiles in this baseline scenario, alpha particle transport losses and redistribution by TAEs is minimal.

M. Fitzgerald, S.E. Sharapov

CCFE Culham Science Centre, Abingdon, Oxon, OX14 3DB, UK

P. Rodrigues, D. Borba

Instituto de Plasmas e Fusão Nuclear, Instituto Superior Técnico, Universidade de Lisboa, 1049-001 Lisboa, Portugal

1. Introduction

The burning plasma experiments to be attempted in ITER will differ from previous experiments in that non-thermal fusion alpha-particles must be satisfactorily confined, both to ensure machine safety, and to attain conditions required for new burning plasma physics studies. These fast fusion alphas have characteristic transit speeds that are comparable with the Alfvén speed, thereby allowing resonant destabilisation of Alfvén normal modes in otherwise magnetohydrodynamic (MHD) stable equilibria[1][2]. Toroidal Alfvén eigenmodes (TAE) are routinely observed in many experiments [3][4] [5][6] in the presence of super-Alfvénic confined species, and in particular, have been driven unstable by alpha-particles in TFTR [7]. Linear studies [8][9] have demonstrated that the ITER Q=10 baseline scenario may be unstable to TAE modes.

To assess the consequences of this instability we may proceed in two ways. Firstly, a succession of stable equilibria preceding our unstable case may be considered to identify the best marginal, and strictly speaking obtainable, stable scenario. Alternatively, if any instabilities encountered are not too violent, then we may obtain a nonlinearly stable asymmetric equilibrium state as a relaxation from the nearby unstable symmetric state. In this study, we take the latter approach to study the nonlinear saturation of the unstable baseline ITER scenario, in order to evaluate the significance of alpha-particle driven TAE modes to the alpha-particle confinement.

2. Scenario equilibrium and modes

Our analysis is conducted on a 2D axisymmetric equilibrium generated with the ASTRA code [10]. Here we briefly summarise the key features of this equilibrium which has been discussed in detail in previous work [11], including figures of mode structure and profiles. We consider plasma parameters and profiles predicted with the ASTRA transport code for the ITER baseline scenario with current $I_p = 15$MA, $R_0 = 6.21$m, $a = 2$m, $q_0 = 0.9859$ and $B_0 = 5.3$T. The model is based on a 2D SPIDER equilibrium for the baseline 2008 separatrix, and the prediction of the plasma profiles is obtained from 1D scaling-based transport for electron and ion temperatures, current density, electron and ion densities. The fuel ion species have deuterium-tritium (DT) mixture close to the optimum ratio 50:50, the density of helium ions resulting from the fusion reactions varies as a function of fusion reactivity, and the beryllium impurity ions coming from the first wall have densities equalling 2% of the electron density. The auxiliary heating and current drive includes two deuterium negative ion NBI sources with energies of 1 MeV and total power 16.5 MW (on-axis)+16.5 MW (off-axis), and with ECRH from the upper launcher aiming at the power deposition in vicinity of $q = 3/2$ and power 6 MW. Energetic alpha-particle and beam populations are produced in ASTRA by solving the linearised Fokker-Planck equation, giving the radial density profile of fast ions. The energy distribution function of alpha-particles is assumed to conform to the slowing down distribution based on the electron and ion temperature values at the magnetic axis: $T_e = 24.7$ keV and $T_i = 21.5$ keV.

It is important to note [11] that almost all alpha-particles are confined within the central region of the plasma, $r/a \leq 0.5$, with the highest gradient of the alpha-particle pressure at $r/a \approx 0.42$. We also emphasise that ion temperature is quite peaked, but electron density profile is very flat up to the edge region of the plasma, $r/a \approx 0.9$. The He ash profile is peaked on-axis, with the DT ion profile depleted on-axis correspondingly.

The baseline sawtoothing scenario in ITER is expected to have flat safety factor profiles $q(r)$ in the plasma core region, with magnetic shear close to zero at $r/a \leq 0.5$. As for the alpha-particle pressure, two very different plasma regions exist with this safety factor profile, the low-shear core region, $r/a \leq 0.5$, and external high-shear region, $0.5 \leq r/a \leq 1$.

For such equilibria, low-shear core-localised TAE (CLTAE) eigenmodes may exist in the plasma core. Since these modes are localised in the region of highest alpha-particle pressure and alpha-particle pressure gradient, they are most strongly driven by the alphas and are most likely to be excited first. However, the radial mode structure of such TAEs consist predominantly of two coupled poloidal harmonics, so the re-distribution of alpha-particles caused by such modes is expected only in the narrow region occupied by the two harmonics. In the external region, the magnetic

shear becomes high and global TAEs can be found, consisting of around 10 poloidal harmonics. These modes are quite extended in radius, and for every toroidal mode number n, many can be found with somewhat different frequencies.

The stability calculations presented in this paper utilise a combination of analytical estimates and the codes MISHKA [12], CASTOR-K [13] and HAGIS [14]. The MISHKA code is a linear MHD solver that is used to provide the TAE eigenmodes for the perturbative drift-kinetic calculations performed with CASTOR-K and HAGIS. The validity of this sort of perturbative approach for TAE modes with small continuum damping can be found in significant detail elsewhere [15]. CASTOR-K computes the imaginary drift-kinetic linear perturbation to the real MHD obtained frequency of the eigenmode. This can provide linear growth rates due to an input fast particle distribution function, but can also be used to compute the thermal species Landau damping. The HAGIS code self-consistently evolves the wave-particle interaction as an initial value problem in time, keeping the MHD eigenmode structure fixed but updating the particle dynamical variables and wave amplitudes and phases. HAGIS has sufficient physics detail to solve the nonlinear trapped particle Landau damping problem [16] for single and multiple modes including associated frequency sweeping in the presence of damped marginal modes [17].

3. Linear drive of modes in the range n=1-35

129 TAE eigenmodes were identified for the range of toroidal mode numbers n=1-35 using MISHKA. The self-consistent evolution of the eigenmodes was computed with HAGIS for each mode, individually in isolation, in the presence of the equilibrium and alpha distribution described earlier. The desired convergence of $\sim \pm 5\%$ in growth rate was achieved with 16000 markers. The time evolution of each mode was fitted by an exponential for the first 20 periods to obtain the normalised linear growth rate well before saturation and are shown in Fig. 1. The values agree well with CASTOR-K results [9] and show the growth rate peaking near n=30, in accord with estimates using the expected orbit width [11]. The even parity eigenmodes are consistently found to have the highest linear drive, with odd parity core localised modes being comparable in drive to some of the external region modes. Part of this trend is attributable to changes in mode frequency, since even parity modes are found at the bottom of the TAE frequency gap and odd modes are found near the top.

4. Nonlinear evolution of Modes 15-35 without damping: coupled versus uncoupled

To understand the nonlinear aspects of the problem, we first carried out HAGIS calculations for core localised modes only in the range n=19-31, without any prescribed damping. Our findings agreed with previous upper-limit calculations for ITER core TAEs using the code 'FAC' [18], the findings being that undamped modes, when uncoupled, reached amplitudes approaching $\delta B_r/B \approx 10^{-3}$, and that redistribution was modest and localised to a small region. We omit these results here.

The FAC study on idealised circular geometry did not cover low toroidal mode number or non-core TAEs. These neglected modes have larger radial extents but were expected to be stable due to strong continuum damping and weaker drive. On inspection of the shear Alfvén continuum in the equilibrium used in this study [11][19],

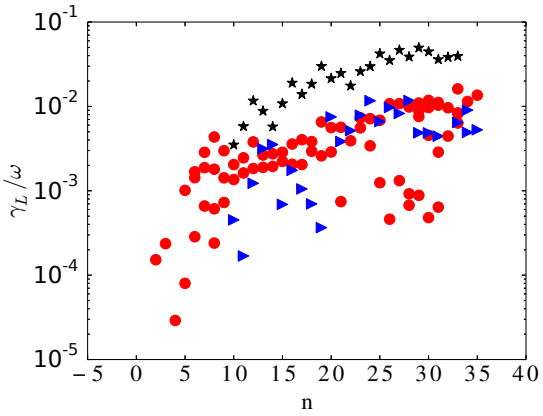

Figure 1: Linear growth rates obtained by fitting to the first 20 wave periods in the absence of damping or coupling. The even parity core localised modes (black star) have higher growth rates than the odd parity core (blue triangle) and external high shear (red circle) modes. The labelling of core and external modes is not done for low mode numbers where such a distinction is not useful.

the TAE gap is open suggesting small coupling to the Alfvén continuum. Thus it is not reasonable to neglect the external modes as categorically stable.

We investigated possible nonlinear avalanche effects [20] between core localised modes and broader TAEs by retaining these broader modes. Our first calculations were limited to 88 modes in the range n=15-35. Fig. 2a shows the growth and nonlinear saturation of all 88 modes evolving separately. The saturation level attained by each mode is in proportion to the linear growth rate, and we have deliberately labeled modes with the same colours as in Fig. 1 to help show this. We will keep this convention for the rest of the paper.

In Fig. 2b, 88 modes in the range n=15-35 are included simultaneously in the one simulation, in the absence of imposed damping. The nonlinear interaction of modes mediated by the alpha population is responsible for all differences from Fig. 2a. The sudden and brief sharp collapses in mode amplitude are typical of such kinetic coupling effects in HAGIS (see for example [21]). Such modulation of amplitude is also expected when damping mechanisms are present for modes in isolation (see for example [17][22]). There is a clear amplification of core localised modes but not of global modes, evident even without letting the simulation reach full saturation. The amplification through coupling calculated at this early unsaturated stage is less than a factor of 10 and in line with previous calculations [23]. One can show by simple geometric arguments that overlapping modes in phase space may release more free energy i.e.: the area under the flattened region of the distribution function for overlapping modes is larger than the sum of areas for isolated modes.

Given the importance of damping, particularly Landau damping, to the ultimate conclusions drawn about stability, here we abandon any further discussion of possible long term evolution of these large undamped modes. It is sufficient for our purposes to have shown that energy exchange between modes is present in the simulation for

our chosen numerical parameters.

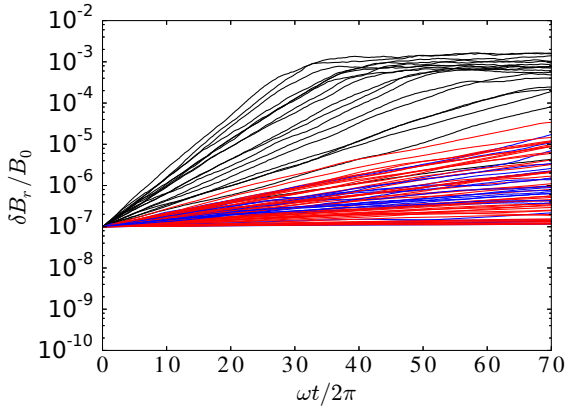

(a)

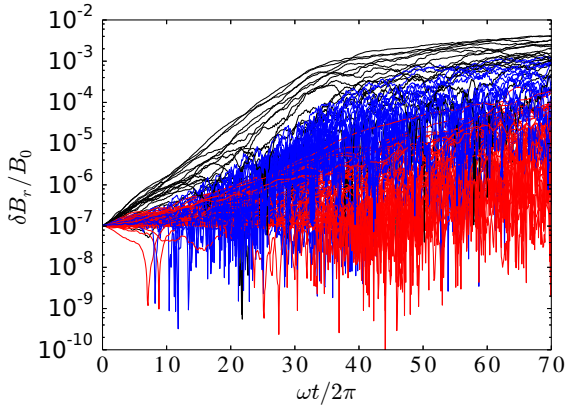

(b)

Figure 2: Growth and saturation of 88 modes n=15-35 uncoupled (a) versus coupled (b). Kinetic coupling between modes is demonstrated, resulting in the amplification of core localised modes. No linear damping rate has been imposed here, resulting in extreme amplitudes for the even parity core modes.

5. Nonlinear simulations of n=15-35 including Landau damping and unlocked phases

5.1. CASTOR-K Landau damping

Estimates for the Landau damping due to thermalised deuterium/tritium, electrons and helium ash were performed with the code CASTOR-K, the details of which may be found in [9]. Although these are detailed drift kinetic calculations using the best available information for geometry and predicted profiles, it should be noted that the

results have an exponential sensitivity to the average ion temperature. For example, the analytical result for thermal deuterium ion Landau damping is [11][24]

$$\frac{\gamma_D}{\omega} \simeq -\frac{\sqrt{\pi}}{4} q^2 \beta_D x_D \left(1 + \left(1 + 2\frac{T_e}{T_D} + 2x_D^2\right)^2\right) \exp\left(-x_D^2\right) \quad (1)$$

$$x_D \equiv V_A / 3V_D \quad (2)$$

where $\beta_D = 2\mu_0 n_D T_D / B_0^2$, V_A is the Alfvén speed, V_D is the thermal speed, and all quantities are evaluated at the TAE radius. For this ITER scenario, a 20% variation in ion temperature can mean a $\sim 50\%$ variation in the ion Landau damping.

5.2. Long coupled simulation

The introduction of damping into the system opens the possibility of phase space hole and clump formation by marginally stable modes [17] when the phase of the modes is allowed to vary. It is conceivable that such structures could carry clumps of alpha particles outwards, thereby adding a coherent convective contribution to the likely stochastic diffusive transport. Experimentation with the HAGIS code numerical parameters leads us to conclude that to properly resolve these hole and clump structures for individual modes requires an order of magnitude more particles than the number required for convergence of growth rate and saturation. The coupled mode HAGIS simulations presented here onwards in this paper have 160,000 particles to resolve these effects if they are present.

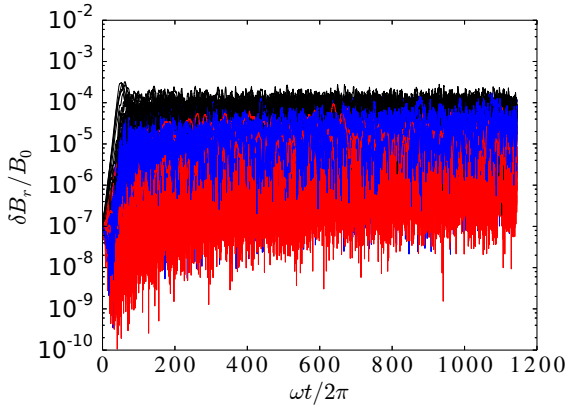

Figure 3: Long simulation of all modes n=15-35 with the inclusion of thermal ion and electron Landau damping, unlocked phases and coupling. The imposition of a linear Landau damping term reduces the maximum amplitude obtained by more than an order of magnitude.

A long simulation was performed with 88 modes in the range n=15-35 with the inclusion of Landau damping as computed by CASTOR-K, over a period of $\sim$ 15ms which corresponds to about 1100 wave periods, depending on which eigenmode is chosen for such a comparison. The evolution of each amplitude is presented in Fig. 3. Again, as for the undamped coupled simulation in Fig. 2b, the core localised modes are

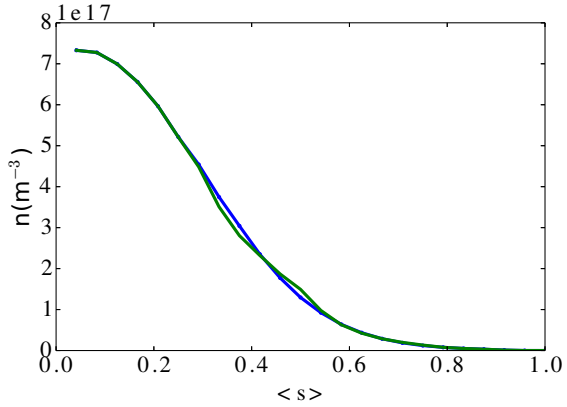

(a)

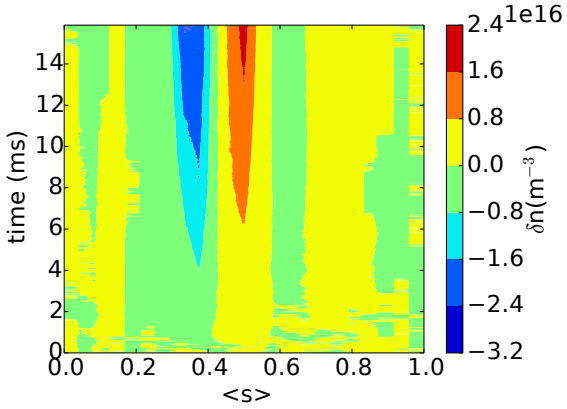

(b)

Figure 4: Self-consistent redistribution of alpha-particles in the n=15-35 long simulation, where $\langle s \rangle$ is the orbit averaged and normalised poloidal flux label $\sqrt{\psi_p}$. The small saturation amplitudes result in a slow removal of stored energy from the surface averaged distribution function (a). This remaining stored energy maintains the saturated amplitude on these timescales. The redistribution of particles is clearly confined to the core region (b) and no avalanche effect with external modes is responsible for additional transport.

more powerful than the external modes and the even-parity modes are strongest. This long simulation with Landau damping included makes fairly clear that no mode under the drive of alpha-particles alone will reach a $\delta B_r/B$ much beyond 10^{-4}. Coupling effects are responsible for the growth and saturation of all linearly stable modes. The blue odd-parity modes can be seen to grow at a slow (i.e.: not exponential) rate after the beginning of the saturation period, which is a reminder that 'saturation' in this context refers to the large departure from initial exponential growth rather than a final maximum, a fact easily overlooked when amplitude is plotted on a logarithmic

scale for short simulations. It is not until all free energy in the resonant region of the distribution function is exhausted that the modes reach true saturation. The initial and final radial alpha density profiles for the long simulation are given in the left of Fig. 4a, and show that it is indeed not the case that the final distribution is flat, which may clarify the nature of the saturation achieved in Fig. 3; the slow growth supplied by the remaining free energy in the distribution function is balanced by the imposed Landau damping in a quasi-steady state. It is expected that once this energy is exhausted, on much longer timescales than simulated here due to slow phase mixing at low amplitudes, then the modes will decay. The time evolution of the redistribution is shown in Fig. 4b, showing that the external high shear TAEs, although present, are not contributing to the transport of core alpha-particles. Because of this, our results broadly repeat the findings of the previous FAC study [18] where the high shear TAEs were neglected. Furthermore, no phase space holes or clumps appear on the density perturbation plot. As mentioned earlier, HAGIS is able to resolve hole and clump formation and the associated sweeping of frequency routinely for single mode simulations for the numerical settings used here. We speculate that although some modes are marginally unstable, the interaction of so many coupled modes in this simulation has led to the breakup of any coherent structures in the neighbourhood of the resonances, making the strongest component of transport stochastic and diffusive.

6. The addition of modes n=10-14 and radiative damping

Subsequent simulations were performed to further scrutinise the basic result that core localised modes are the only modes that contribute to alpha driven TAE redistribution. On the basis of linear growth rate, lower n TAEs were expected to be less strongly driven, but the possibility of nonlinear drive remained as a mechanism for further transport. It was supposed that the larger radial extents of the low n modes could play a role in extending alpha transport beyond the core region. 108 modes between n=10-35 were the subject of further simulation. In addition, it was expected that even-parity core localised modes would have significant radiative damping [11] [19][9]. The analytical estimate for radiative damping was found to give a value of $\gamma_d/\omega = 1.3\%$, and this was imposed on the even CLTAEs in addition to Landau damping. Neither the addition of radiative damping, nor the further inclusion of modes n=10-14 changed the findings of the previous simulation in a substantial way, and for the sake of brevity, we omit repeating what are essentially the same figures as before, although for a shorter simulation time and a slightly lower saturation level, due to the addition of radiative damping.

6.1. Stochasticity

The limited radial transport of the alpha-particles may be clarified by examining test-particle orbits in the presence of the saturated TAE eigenmodes at the end of the n=10-35 simulation. Three deeply passing ($\Lambda \equiv \mu B_0/E = 0$) test particle orbits for the same energy of 981keV ($\approx 1.2 \times v_A$ on axis) were computed, and were chosen at precise radial locations so that they were resonant. The large number of modes gave some freedom in where these radial positions could be chosen, therefore particles were placed among the core modes, among the external modes, and in a weaker perturbed region in between.

Fig. 5a is a Poincaré plot of the three test-particle orbits super-imposed onto a

plot of magnitude of the perturbed TAE field, and Fig. 5b are the corresponding plots of the canonical toroidal momentum for each orbit using only the equilibrium field $P_\zeta = g(\psi)mv_\parallel/B - Ze\psi$. Considering for a moment only the perturbed fields, the very centre can be seen to be completely devoid of activity due to the lack of TAE eigenmode solutions in that region where $q \approx 1$. Turning attention to the particle orbits, the particle resonating with the core localised TAEs undergoes the strongest transport, giving a stochastic region radial width of 7cm. In contrast, the external modes produce only 1cm deviation in its test particle, and the intermediate orbit is approaching deviations of 1mm.

We therefore conclude that resonant particles in the three different regions undergo significantly different radial diffusion, and the limited radial redistribution of particles we observe in our nonlinear simulations, Fig. 4b, may be understood in terms of a transport barrier in the quiet region of TAE activity between the core and external modes. This transport barrier is a consequence of the low shear core q profile in this Q=10 baseline scenario, and the expected low saturation levels attained by TAEs when Landau damping is taken into account. The resilience of this transport barrier to errors in predicted mode amplitudes may be demonstrated by artificially increasing the mode amplitudes and seeing what happens to the test particle orbits. Fig. 5c and Fig. 5d are the corresponding plots for test particles when the mode amplitudes are uniformly scaled up by a factor of 50. The stochastic radial widths for both core and external orbits have reached over 50cm, but the core orbit is very clearly still confined to the core region. Additionally, a particle free region of a few centimetres is discernible on the Poincaré plot. The transport barrier breaks down before the scaling reaches a factor of 100 (not shown). These artificially scaled mode amplitudes are at levels attainable only when damping is completely neglected, such as Fig. 2b. Indeed, such artificially high TAE mode amplitudes in the range $\delta B_r/B \sim 1 \times 10^{-2}$ would cause more basic concerns for stability, the validity of linear TAE eigenmodes, and the integrability of orbits. Therefore, for the baseline scenario, we expect that only simulations which neglect all damping will see large radial diffusion due to avalanche effects overcoming this transport barrier.

7. All modes 1-35

The final results presented here are the result of a further many-mode simulation containing 129 modes found in the range n=1-35 with damping. The modes from n=1-10 are interesting in that the distinction between core and external modes is ambiguous. If these modes could be driven to large saturation amplitudes, then the radial transport barrier found earlier could be overcome. To discount this possibility we completely neglected damping for modes in the range n=1-10, whilst keeping Landau and radiative damping for modes n=10-35. The coupled amplitude evolution for the 129 modes is presented in Fig. 6a. We remind the reader of the colouring convention used in this paper, with even parity core modes being strongest, followed by odd parity core modes, and external modes being weakest. The additional low mode number eigenmodes are now visible as red incursions in previously exclusively black and blue regions, partially due to lack of damping, and partially due to the lack of distinction between core and external nature of these modes. Even with the inclusion of low toroidal mode number eigenmodes, a separation in TAE activity between core and external modes is still quite clearly discernible for the final perturbation state of the simulation plotted in Fig. 6b. The time evolution of perturbed density plotted

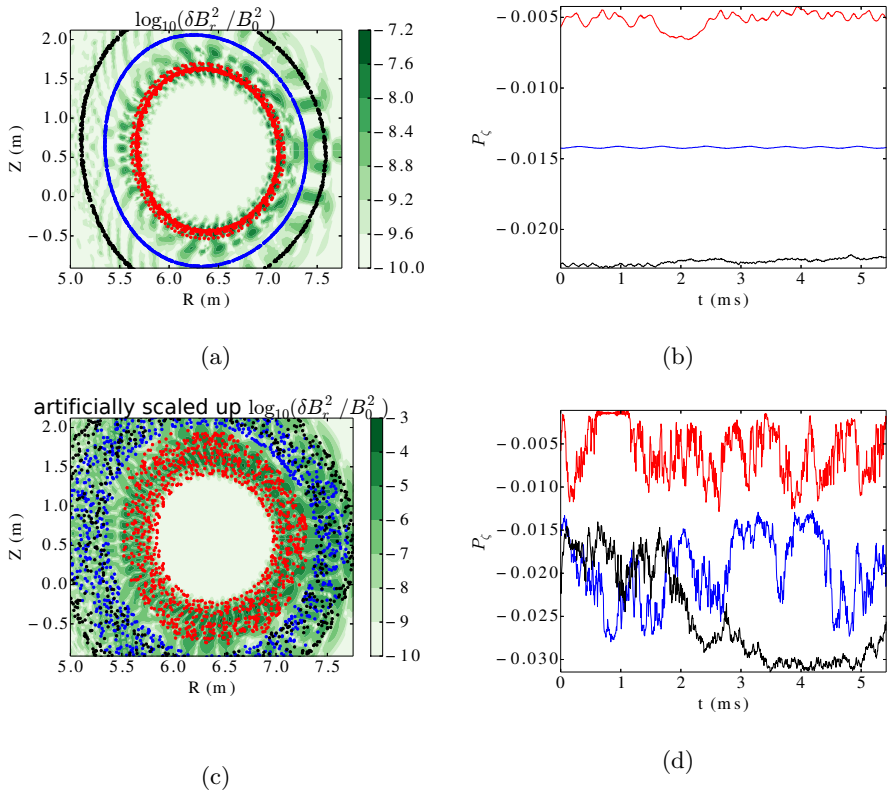

Figure 5: Deeply passing resonant test particle Poincaré maps (blue, black and red) overplotted on TAE activity (green) in figure (a), and the corresponding evolution in canonical momentum (b). The fields obtained in the first two graphs are for a long simulation with additional modes (now all modes n=10-35) and the inclusion of radiative damping on the even parity core modes. A clear transport barrier is established in the quiet region between the core modes and the external modes. This barrier is still evident in (c) and (d), where the saturation amplitudes have been artificially increased by a factor of 50. The barrier breaks down completely somewhere between scaling of 50 and 100 (not shown). Fourier transforms of the time traces of P_ζ in (d) were found to follow a $1/f$ 'pink noise' spectrum.

in Fig. 6c is largely unchanged from Fig. 4b, supporting this notion. At time of publication, damping rates for the low mode number TAEs were not available and we expect the alpha-particle confinement conclusions herein to not vary significantly with their reintroduction.

8. Conclusion

We have presented computations on the nonlinear aspects of the TAE-alpha-particle interaction on a realistic Q=10 baseline scenario, making predictions on the magnitude and extent of alpha-particle redistribution due to alpha-particle spatial gradients in the presence of modes n=1-35. When realistic Landau and radiative damping is included

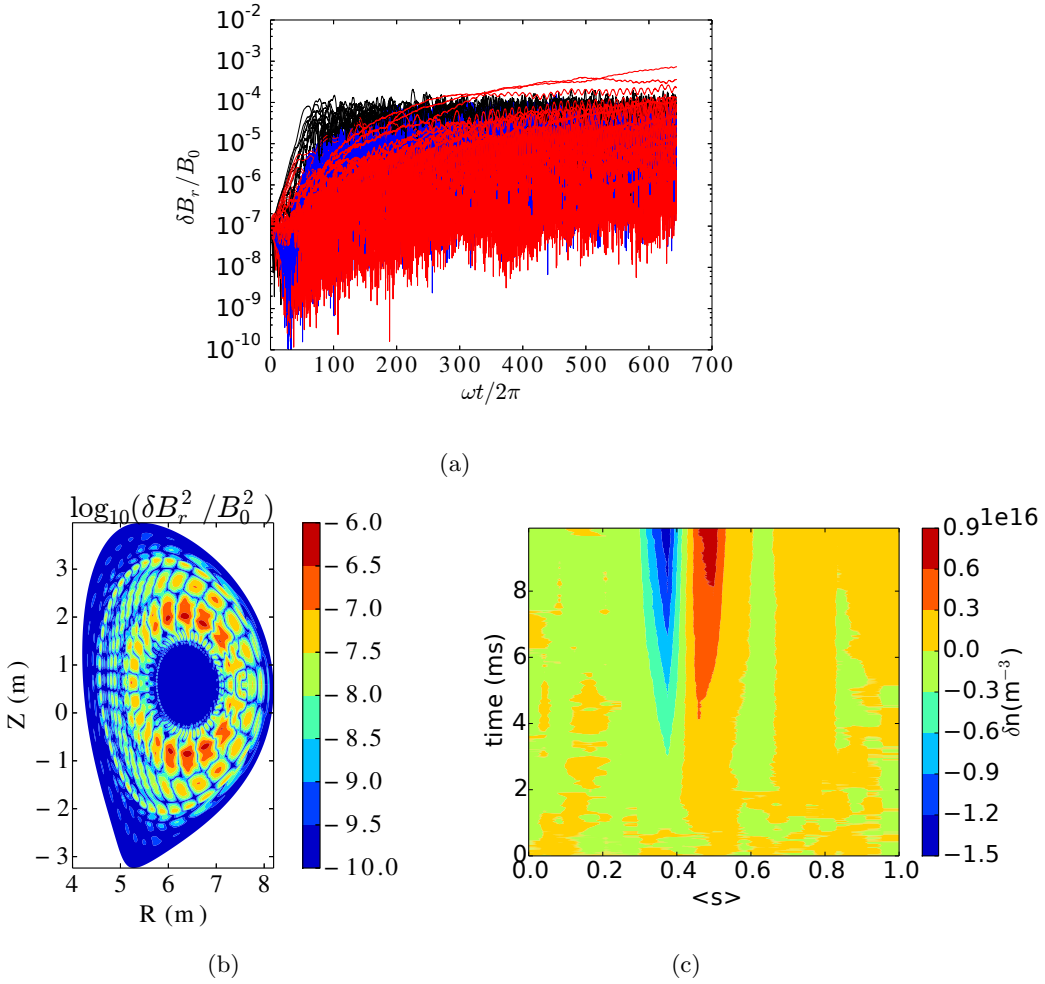

Figure 6: 129 mode simulation of $n = 1 - 35$ including the effects of Landau damping and radiative damping for $n \geq 10$. Global low toroidal mode number eigenmodes are not able to overcome the transport barrier.

in the coupled evolution of the TAE modes, the modes reach amplitudes approaching $\delta B_r/B \approx 3 \times 10^{-4}$, with core modes being the largest. Radial transport is limited to a few centimetres near the core localised modes.

The super-Alfvénic neutral beams and the potential error bar in damping predictions mean that some caution should be exercised in ruling out alpha-particle redistribution in this scenario. However, we have shown that avalanche effects, which are required to produce large radial transport, are significantly suppressed by a transport barrier which is resilient to amplitude increases by a factor of 50 over our computed saturation levels. It is difficult to see how the addition of neutral beam drive, and an evolution to marginal stability, will materially overcome this basic feature of the magnetic geometry. Perhaps the synergy with another unrelated effect, such as an energetic particle mode or reconnection event, could alter this conclusion, but the

more obvious line of enquiry now for ITER TAE induced instability is to explore sensitivity to changes in q-profile and magnetic shear.

9. Acknowledgments

Our thanks go to Simon Pinches and Alexei Polevoi (ITER) and other members of the ITPA Energetic Particle Physics Topical Group, for providing the baseline scenario equilibrium, and to Philip Lauber and Mirjam Schneller (IPP Garching) for drawing our attention to low mode numbers. PR was supported by EUROfusion Consortium grant no. WP14-FRF-IST/Rodrigues. This work has been carried out within the framework of the EUROfusion Consortium and has received funding from the Euratom research and training programme 2014-2018 under grant agreement No 633053 and from the RCUK Energy Programme [grant number EP/I501045]. The views and opinions expressed herein do not necessarily reflect those of the European Commission.

[1] M N Rosenbluth and P H Rutherford. Excitation of Alfven waves by high-energy ions in a tokamak. *Physical Review Letters*, 34(23):1428–1431, 1975.

[2] A B Mikhailovskii. Thermonuclear 'drift' instabilities. *Soviet Physics JETP*, 1782(May 1975):890–894, 1976.

[3] S Ali-Arshad and D J Campbell. Observation of TAE activity in JET. *Plasma Physics and Controlled Fusion*, 37(7):715–722, July 1995.

[4] W Kerner, D Borba, S E Sharapov, B N Breizman, J Candy, A Fasoli, L C Appel, R Heeter, L G Eriksson, and M J Mantsinen. Theory of Alfvén eigenmode instabilities and related alpha particle transport in JET deuterium-tritium plasmas. *Nuclear Fusion*, 38(9):1315–1332, September 1998.

[5] H H Duong, W W Heidbrink, E J Strait, T W Petrie, R Lee, R A Moyer, and J G Watkins. Loss of energetic beam ions during TAE instabilities. *Nuclear Fusion*, 33(5):749–765, 1993.

[6] King-lap Wong. A review of Alfvén eigenmode observations in toroidal plasmas. *Plasma Physics and Controlled Fusion*, 41(1):R1–R56, January 1999.

[7] R Nazikian, G Y Fu, S H Batha, M G Bell, R E Bell, R V Budny, C E Bush, Z Chang, Y Chen, C Z Cheng, D S Darrow, P C Efthimion, E D Fredrickson, N N Gorelenkov, B Leblanc, F M Levinton, R Majeski, E Mazzucato, S S Medley, H K Park, M P Petrov, D A Spong, J D Strachan, E J Synakowski, G Taylor, S VonGoeler, R B White, K L Wong, and S J Zweben. Alpha-particle-driven toroidal Alfven eigenmodes in the tokamak fusion test reactor. *Physical Review Letters*, 78(15):2976–2979, 1997.

[8] G Y Fu and J W Van Dam. Excitation of the toroidicity-induced shear Alfven eigenmode by fusion alpha particles in an ignited tokamak. *Physics of Fluids B: Plasma Physics*, 1989.

[9] P Rodrigues, A Figueiredo, J Ferreira, R Coelho, F Nabais, D Borba, N F Loureiro, H J C Oliver, and S E Sharapov. Systematic linear-stability assessment of Alfvén eigenmodes in the presence of fusion α-particles for ITER-like equilibria. *Nuclear Fusion*, 55(8):083003, August 2015.

[10] A Polevoi, S Medvedev, V Mukhovatov, A Kukushkin, Y Murakami, M Shimada, and A Ivanov. ITER confinement and stability modelling. *J. Plasma Fusion Research, SERIES*, 5:82–87, 2002.

[11] S D Pinches, I T Chapman, Ph W Lauber, H J C Oliver, S E Sharapov, K Shinohara, and K Tani. Energetic ions in ITER plasmas. *Physics of Plasmas*, 22:021807, 2015.

[12] A B Mikhailovskii, G T A Huysmans, W O K Kerner, and S E Sharapov. Optimization of computational MHD normal-mode analysis for tokamaks. *PLASMA PHYSICS REPORTS*, 23(10):844–857, October 1997.

[13] D Borba, H L Berk, B N Breizman, A Fasoli, F Nabais, S D Pinches, S E Sharapov, and D Testa. Modelling of Alfvén waves in JET plasmas with the CASTOR-K code*. *Nuclear Fusion*, 42(8):1029–1038, August 2002.

[14] S D Pinches, L C Appel, J Candy, S E Sharapov, H L Berk, D Borba, B N Breizman, T C Hender, K I Hopcraft, G T A Huysmans, and W Kerner. The HAGIS self-consistent nonlinear wave-particle interaction model. *Computer Physics Communications*, 111(1-3):133–149, June 1998.

[15] H L Berk, J W Van Dam, Z Guo, and D M Lindberg. Continuum damping of low-n toroidicity-induced shear Alfven eigenmodes. *Physics of Fluids B: Plasma Physics*, 4(7):1806, 1992.

[16] Thomas O'Neil. Collisionless Damping of Nonlinear Plasma Oscillations. *Physics of Fluids*, 8(1965):2255–2262, 1965.

[17] H L Berk, B N Breizman, and M Pekker. Nonlinear Dynamics of a Driven Mode near Marginal Stability. *Physical Review Letters*, 76(8):1256–1259, February 1996.

[18] J Candy, D Borba, H L Berk, G T A Huysmans, and W Kerner. Nonlinear interaction of fast particles with Alfven waves in toroidal plasmas. *Physics of Plasmas*, 4(7):2597, 1997.

[19] Ph Lauber. Local and global kinetic stability analysis of Alfvén eigenmodes in the 15 MA ITER scenario. *Plasma Physics and Controlled Fusion*, 57(5):054011, May 2015.

[20] M Schneller, Ph Lauber, R Bilato, M García-Muñoz, M Brüdgam, and S Günter. Multi-mode Alfvénic fast particle transport and losses: numerical versus experimental observation. *Nuclear Fusion*, 53(12):123003, December 2013.

[21] T Gassner, K Schoepf, S E Sharapov, V G Kiptily, S D Pinches, C Hellesen, and J Eriksson. Deuterium beam acceleration with 3rd harmonic ion cyclotron resonance heating in Joint European Torus: Sawtooth stabilization and Alfven eigenmodes. *Physics of Plasmas*, 19(3):32115, March 2012.

[22] H Vernon Wong and H L Berk. Growth and saturation of toroidal Alfven eigenmode modes destabilized by ion cyclotron range of frequency produced tails. *Physics of Plasmas*, 5(7):2781, 1998.

[23] Simon David Pinches. *Nonlinear Interaction of Fast Particles with Alfven Waves in Tokamaks*. PhD thesis, University of Notingham, 1996.

[24] R Betti and J P Freidberg. Stability of Alfven gap modes in burning plasmas. *Physics of Fluids B: Plasma Physics*, 4(6):1465, 1992.